Fabrication of polypropylene membrane via thermally induced phase separation as a support matrix of tridodecylamine supported liquid membrane for Red 3BS dye removal

Norasikin Othman*, Norlisa Harruddin, Ani Idris, Zing-Yi Ooi, Norul Fatiha, Raja Norimie Raja Sulaiman

Faculty of Chemical Engineering, Centre of Lipid Engineering and Applied Research (CLEAR), Department of Chemical Engineering, Universiti Teknologi Malaysia, 81310 UTM, Skudai, Johor Bahru, Malaysia, Tel. +60 7 5535561; Fax: +60 7 5581463; emails: norasikin@cheme.utm.my (N. Othman), norlisaharruddin@gmail.com (N. Harruddin), ani@cheme.utm.my (A. Idris), ozyi88@hotmail.com (Z.-Y. Ooi), norulfatiha.mn@gmail.com (N. Fatiha), rajanorimie_0804@yahoo.com (R.N. Raja Sulaiman)

ABSTRACT

The separation of reactive Red 3BS ions across supported liquid membrane (SLM) process using tridodecylamine as a carrier and sodium hydroxide as a stripping agent was studied. A microporous polypropylene membrane fabricated using thermally induced phase separation technique was used as a membrane support for the SLM process. Three polymer concentrations (10, 15, and 20 wt%) and two quenching temperatures (7 and 29°C) were applied for the polymer-diluent solution. The results demonstrated that all membranes appeared with similar morphologies but different in pore size and porosity. The membrane with 15 wt% polymer concentration quenched at 29°C produced a microporous membrane with a symmetric structure, defined pore size, and performed high stability toward reactive dye extraction, thus feasible to be used as the support material. This membrane had successfully removed and recovered almost 100 and 58% of Red 3BS from an aqueous solution, respectively. Besides, it also exhibited high stability up to 25.5 h of extraction, hence demonstrating an improved performance for the separation of reactive dyes using SLM process.

Keywords: Reactive dye; Supported liquid membrane; Thermal induced phase separation; Fabricated membrane

1. Introduction

Reactive dyes are mainly used in textiles industry due to their favorable characteristics such as bright color, water fastness, and formation of strong interactions with fabrics. These kinds of features are due to their complex chemical structure containing benzidine ring substituent of azo coupling to aromatic system and the presence of other aromatic amine compounds as discussed by Mathur et al. [1]. However, the presence of reactive dyes in wastewater causes destruction to mankind and environment [2]. According to Kadirvelu et al. the discharge of dyes into water effluent can lead to great damage toward human body, reproductive system, and functional failure of kidney, liver, brain, and nervous system [3]. As a consequence, the release of dyes into water bodies resulted in severe impact to the human community and direct destruction

*Corresponding author.

of the aquatic community. Previously, a few techniques have been developed in order to extract reactive dyes from wastewater. One of the methods is liquid–liquid extraction as reported by Othman et al. for the extraction of black B dye using tridodecylamine (TDA) as an extractant [4]. After that, the emulsion liquid membrane process was developed for removal of turquoise blue reactive dye [5] and emulsion liquid membrane process for removal of Red 3BS reactive dye [6]. From these studies, the results are very promising for industrial use. However, the liquid membrane formulation and operating conditions should be managed properly to overcome the emulsion stability problem. The main advantage of liquid membrane configuration treatment is a single-step process, in which the removal and recovery processes occur simultaneously, hence avoiding the production of new solid waste after the removal process. Another alternative mode of liquid membrane technology is supported liquid membrane (SLM) process. This technique also provides high separation efficiency and selectivity toward desired solute as reported by Bukhari et al. [7]. Despite having many potential advantages, SLM has not often been applied in a large scale because it suffers from tremendous problem, namely membrane instability as reported by Kocherginsky et al. about recent advances in SLM technology, in the study of Cobalt (II) transport [8,9], and also in a review paper on facilitated oxygen transport by Figoli et al. [10]. These instability phenomena occur when the liquid membrane fails to be retained in the pore of membrane support, thus leading to carrier lost as reported by Arslan et al. [11].

Membrane support is one of the factors that influence the stability and performance of SLM process. According to Kocherginsky et al. and Dzygiel and Wieczorek, the stability and lifetime process in SLM is greatly influenced by the morphology of membrane since the liquid membrane is held within the pores of the membrane by capillary force [9,12]. New approaches have been taken for enhancing the stabilization of SLM process by fabricating membrane support using thermally induced phase separation (TIPS) technique. TIPS is a well-known process because of its versatility and it is the simplest technique for producing porous membrane support, and it is believed to have the ability to produce membrane with suitable morphology for SLM process as reported by Fu et al. [13]. Besides, the morphology of the membrane also depends strongly on the fabrication condition, phase separation behavior, and thermodynamic interaction between polymer and diluents.

In previous studies of SLM process, only commercial membranes were used as the membrane support for removal of reactive dyes. To the best of our

knowledge, no work has been reported on the preparation of membrane support for removal of reactive dyes from simulated wastewater. Therefore, in this study, the membrane support was fabricated using TIPS method induced by liquid–liquid (L–L) phase separation by varying two experimental parameters, which are type of polymer concentration and quenching condition. The fabricated membrane was tested as a membrane support in SLM process.

2. Materials and methods

2.1. Materials

In order to fabricate a microporous membrane, isotactic polypropylene (iPP) pellets (Mw: 250,000), and diphenyl ether (DPE) were used as a polymeric support and a diluent, respectively. Methanol was chosen as the extractant. All chemicals were procured from Sigma–Aldrich. The properties of iPP, DPE, and methanol are tabulated in Table 1.

Remazol Red 3BS in a powdered form as the targeted solute was obtained from Nozi Batik, Terengganu. The chemical structure, molecular weight, molecular size, and maximum wavelength of Red 3BS are shown in Table 2. For the SLM process, TDA (Merck, 95% purity) was used as a carrier and salicyclic acid (SA) (Fisher Chemical, 99.99% purity) as a co-carrier. Reagent grade kerosene (Fluka, 78% purity) was used as an organic diluent, whereas sodium hydroxide (NaOH) was used as a stripping agent.
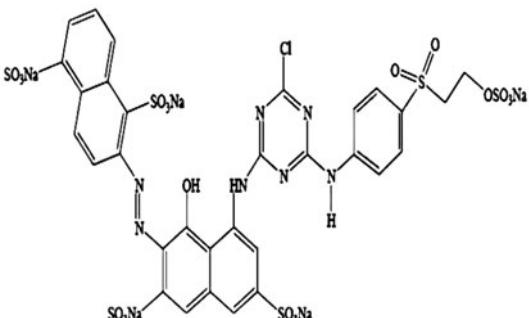
2.2. Fabrication of membrane support via TIPS method

The polypropylene (PP) membrane was fabricated using TIPS method. This method is almost similar to the previous study, but a certain modification step has been proposed in order to produce the desired morphology of membrane [14]. The homogeneous polymer-diluent sample was prepared by dissolving iPP and DPE in a beaker at different polymer concentrations (10, 15, and 20 wt%), and the beaker was purged with nitrogen gas and sealed with an aluminum foil to prevent oxidation. The mixture was then heated on a hot plate at a temperature of 200°C for almost 3 h and continuously stirred until a homogeneous mixture solution appeared. After that, the polymer-diluent solution was cooled at room temperature until it formed a white solid polymer. The white solid polymer was sliced into desired pieces and placed in between two glass plates with a thickness of 0.3 cm and the width of 10 cm to avoid the evaporation of diluent. The thickness of the polymer solution was adjusted to 100 μm by inserting a Teflon film in the

Table 1
Properties of iPP, DPE, and methanol

Properties	iPP	DPE	Methanol
Physical appearance	White pellet	Yellow liquid	Colorless liquid
Melting point (°C)	171	27.5	−98
Boiling point (°C)	Not applicable	258	65

Table 2
Properties of Remazol Red 3BS [14]

Chemical structure	Molecular weight (g/mol)	Molecular size (nm)	λ_{max}
	1,085	1.2	511

square opening of the glass plate. Fig. 1(a) exhibits the apparatus used in the membrane fabrication.

After that, the glass plate containing the solid polymer was remelted in an oven at 200°C for 5 min for melt-blending. Then, the sample was quenched at two different quenching temperatures, either at 7 or 29°C in a horizontal position. According to Fu et al. the different quenching temperatures considerably affect the time for coarsening the droplets in the L–L separation [13]. After the L–L separation had been induced, the membrane was immersed in methanol for one day to extract the diluent and the consequent evaporation of methanol produced microporous membrane.

2.3. Membrane characterization

2.3.1. Porosity measurement

The dry membrane was weighed (w_0). After that, it was immersed in an oil solution. The wet surface of the membrane was wiped using a filter paper and weighed (w_1) again. The membrane porosity (p) was calculated using Eq. (1).

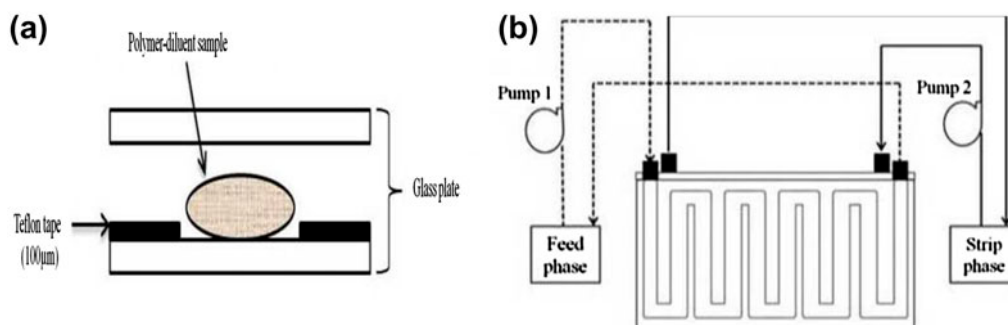$$P = \frac{W_1 - W_0}{Ah} = \frac{V_{pores}}{V_{total}} \times 100 \tag{1}$$

Fig. 1. (a) Apparatus for membrane preparation, (b) schematic diagram of SLM.

where w_1 is the wet sample weight (g), w_0 is the dry sample weight (g), A is the membrane area (cm^2), and h is the membrane thickness (cm).

2.3.2. Membrane structure

Samples were immersed in liquid nitrogen, which generally gives a clean break and their morphologies were viewed with a scanning electron microscope (SEM) Philips XL 4.0.

2.4. SLM process

2.4.1. Preparation of solutions

SLM consists of three phases, which are the feed phase, the liquid membrane phase, and the strip phase. Several screenings were done in the previous study to find an optimum condition for the separation of reactive dye. For the feed phase, 50 ppm of Red 3BS (pH 3) was used as the best condition since it induced the formation of anionic dye ions and complexation between cationic carrier, TDA, and anionic dye, Red 3BS. For the strip phase, 0.1 M NaOH as a stripping agent was sufficient to strip Red 3BS dye ions. For the liquid membrane phase, 0.1 M TDA and 0.1 M SA were dissolved in the kerosene. The formulation of liquid membrane was originally found by Othman et al. using ELM process and was used throughout the experiment [15]. Even though SLM and ELM are categorized under different configurations, but the formulation of liquid membrane is valid for both systems since they used similar types of carrier, which is the highly selective separation for specific solutes as reported by De Agreda et al. [16].

2.4.2. Extraction and recovery process by SLM

The fabricated PP membrane was impregnated in liquid membrane solution for almost 24 h. It was assumed that all the empty voids were filled with the liquid membrane phase. A filter paper was used to remove the excess liquid on the membrane surface. Then, the PP membrane was placed and clamped between two compartments of membrane cell, which consisted of 150 mL of feed and strip phases separated by a liquid membrane phase. Fig. 1(b) shows the experimental setup for the separation of Red 3BS through SLM process. The flow rate of the feed phase and the strip phase was fixed to 100 and 50 mL/min throughout experiments, respectively. All experiments were performed at ambient temperature.

The concentration of Red 3BS was determined by a UV spectrophotometer at the wavelength of 511 nm as a function of time.

2.5. Removal and recovery performance and membrane permeability

2.5.1. Determination of removal and recovery performance

The percentage of removal and recovery of reactive dye ions during the extraction process was calculated using Eqs. (2) and (3).

$$\text{Removal } (\%) = \frac{[\text{Dye}]_{\text{fi}} - [\text{Dye}]_{\text{fo}}}{[\text{Dye}]_{\text{fi}}} \times 100\,\% \qquad (2)$$

$$\text{Recovery } (\%) = \frac{[\text{Dye}]_{\text{s}}}{[\text{Dye}]_{\text{fi}}} \times 100\,\% \qquad (3)$$

where,

$[\text{Dye}]_{\text{fi}}$ is the initial concentration of dye ions in the feed phase,

$[\text{Dye}]_{\text{fo}}$ is the final concentration of dye ions in the feed phase, and

$[\text{Dye}]_{\text{s}}$ in the concentration of dye ions in the strip phase at given time.

The concentration of Red 3BS was measured using UV spectrometer with wavelength of 511 nm.

2.5.2. Determination of permeability value

Membrane permeability is the ability of a substance to allow the desired solute to pass through it. Permeability, p (ms^{-1}) of the dye ions transferred from the feed phase to the strip phase can be determined by Eq. (4):

$$P = \frac{dC}{C} \cdot \frac{1}{dt} \cdot \frac{V}{A} \qquad (4)$$

By integration of Eqs. (4) and (5) was obtained:

$$\ln \frac{C}{C_{\text{fi}}} = -\left(\frac{A}{V}\right) P \times t \qquad (5)$$

where C_{fi} is the initial concentration of Red 3BS in the feed phase and C is the concentration of Red 3BS at given time. Meanwhile, A is the effective area of membrane (cm^2) and V is the volume of aqueous feed phase (cm^3).

2.6. Performance of fabricated membrane

The performance of fabricated membranes with different concentrations of polymer and quenching conditions were tested under favorable condition of SLM process. The favorable condition for SLM process was obtained from the previous study with the flow rate of 100 mL/min, pH 3 of the feed phase, 0.1 M of NaOH, 50 ppm of Red 3BS, and 0.00001 M of sodium silicate. Liquid membrane contained TDA and SA in kerosene with the concentration stated in previous research [15]. The transportation efficiency and membrane permeability were observed every 30 min for 6 h.

3. Results and discussion

3.1. Morphologies of the fabricated membrane support

The morphologies of the membrane obtained from the thermal separation process reflect the thermodynamics and phase separation kinetics of the polymer-diluent solution. Fig. 2 illustrates the SEM micrograph of a whole cross section of iPP membrane at different polymer concentrations and quenching temperatures. Based on the result obtained, all iPP membranes exhibited identical morphologies, similar pore shapes and exhibited a symmetric structure from the top to
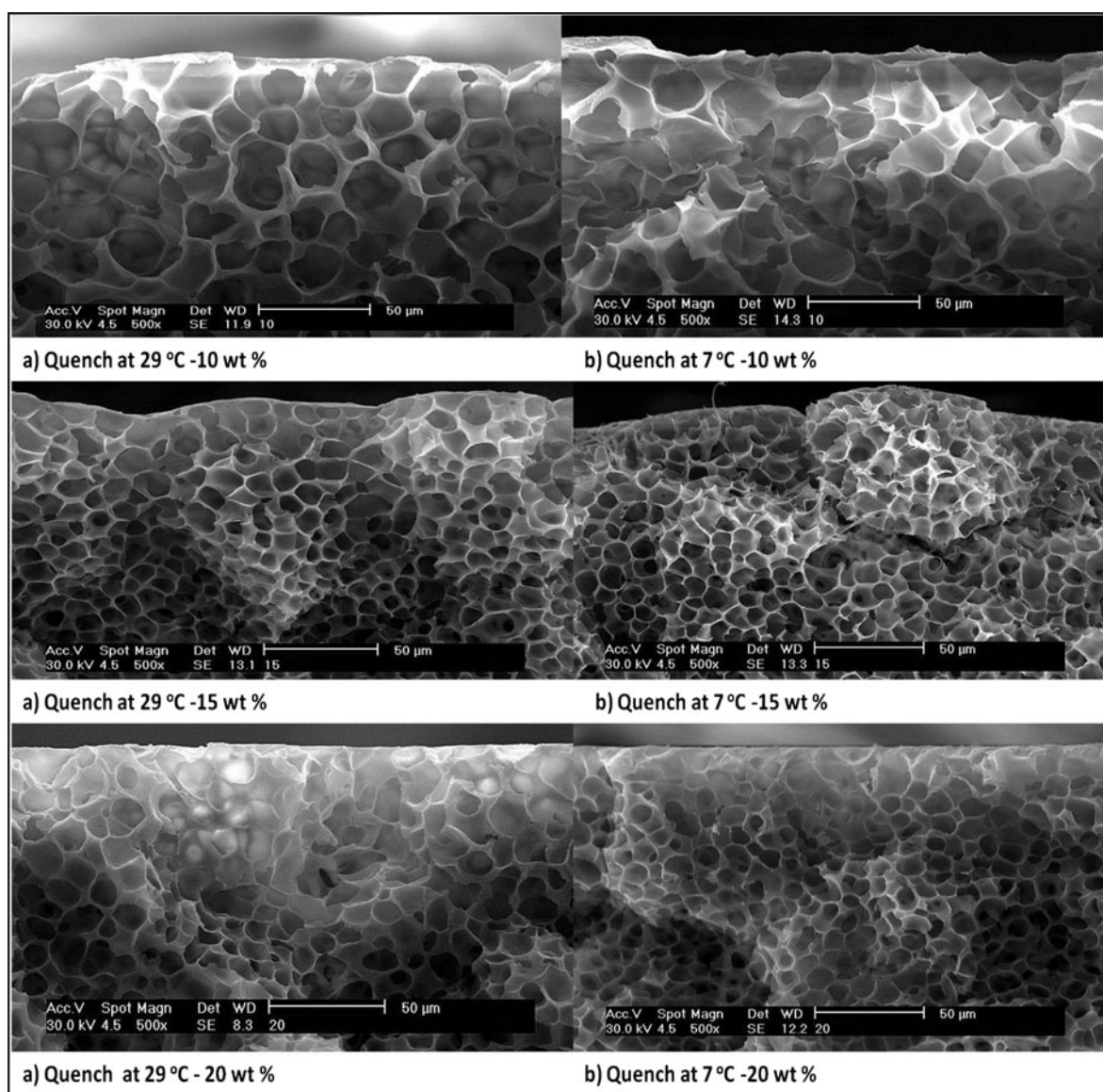

Fig. 2. SEM micrograph of whole cross section of iPP membranes: (a) quench at 29℃—10, 15, and 20 wt% polymer concentration, (b) quench at 7℃—10, 15, and 20 wt% polymer concentration.

the bottom part of the membrane. Symmetric structure is known as the membrane with a uniform structure, defined and fixed pore size throughout the membrane. Commonly, a symmetric membrane is suitable for the SLM process because it has higher stability compared to an asymmetric membrane and it has been explained by Lv et al. in the study of heavy metal ions trans-membrane flux enhancement through SLM [17]. Yang et al. also reported the development of chemically modified P84 Co-polyimide membranes as SLM [18]. According to Lv et al. a force exerted on both sides of the symmetric membranes is almost similar, thus there is a possibility for the improvement of the SLM process [17]. Meanwhile, according to Fu et al. almost 100% of the metal ions were removed using a microporous membrane with a symmetric structure as a support material [19]. The two major factors that control the size of the diluent droplet and shape of diluent rich phase in L–L phase separation are the polymer concentration and the quenching condition. Hence, the noticeable difference in membrane morphologies and pore structure was investigated between three different polymer concentrations and two quenching temperatures.

3.1.1. Effect of polymer concentration on the morphology and porosity of membrane

In order to investigate the effect of polymer concentration, the quenching temperature was fixed at 29℃ to avoid any disruption effect. Fig. 3 shows the SEM micrograph of the cross-section morphology of iPP prepared using different polymer concentrations ranging 10, 15, and 20 wt%. It can be observed that when the polymer concentration increased from 10 to 20 wt%, the interconnectivity between cellular pores and pore size throughout the membrane decreased. It can be observed that membrane (C) has a thicker wall and smaller diameter of pore membrane compared to membrane (A) and (B) due to the high concentration of polymer. Polymer concentration considerably affects the final morphology of the membrane, where the
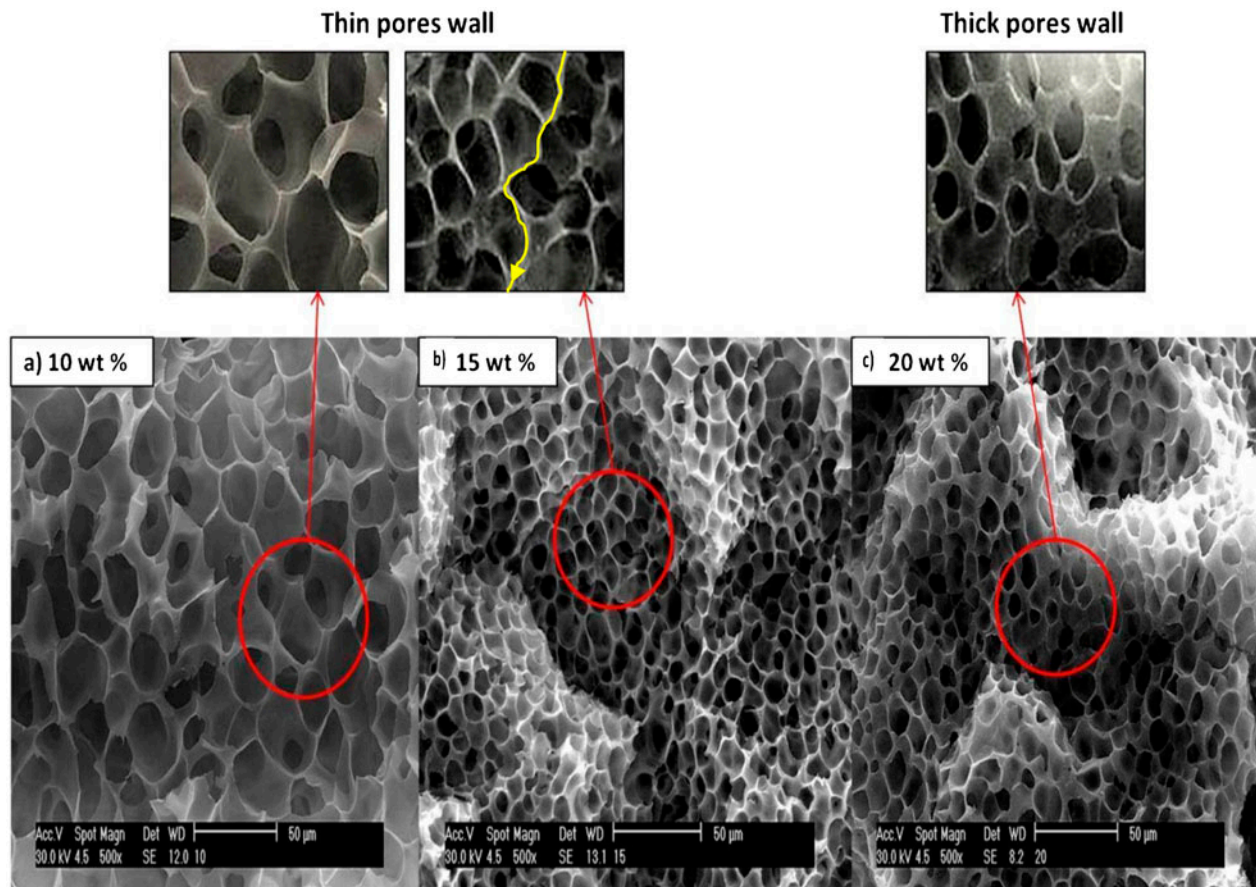

Fig. 3. SEM micrograph of inner cross section of iPP membrane as a function of concentration polymer membrane quench at 29℃: (a)10, (b) 15, and (c) 20 wt%.

Table 3
Pore size and porosity of membrane at different polymer concentration quench at 29°C

Membrane	Polymer concentration (wt%)	Pore size (μm)	Porosity (%)
(a)	10	17.4	93
(b)	15	11.5	85
(c)	20	9.01	85

interconnectivity of pores increased with the decrease in polymer concentration, which leads to the low tensile strength in the polymer-diluent system as reported by Lin et al. in the study of iPP membranes formation with bicontinuous structure via TIPS method and Khayet and Matsuura in the overview of membrane distillation [14,20].

Different polymer concentrations resulted in different pore sizes of the membrane. Table 3 presents the pore size at different polymer concentrations of membrane as shown in Fig. 3. It is shown that an average pore size decreased with the increase in polymer concentration from 10 to 20 wt%. Membrane (a) has larger cellular pores with an average pore size of 17.4 μm, whereas membrane (B) produced slightly small pore size with 11.5 μm, and membrane (C) exhibited closed pore structures with smaller average pore size of 9 μm. The decrement in the pore size upon increasing the polymer concentration can be attributed to the growth rate and viscosity of polymer solutions. Basically, high polymer concentration contributes to high viscosity of the polymer solution, hence reducing the droplet growth rate of pore membrane. The lower droplet growth rate means that the rate for the widening process of pore size is lower, which consequently produces small pore size. This finding is in agreement with Wu et al. in the research about structure and performance of polyacrylonitrile membranes and Sun et al. in the study of impact factors of polymer rheology in porous media [21,22].

Polymer concentrations also influence the overall porosity of the structure [23]. Table 3 exhibits the porosity value of the membrane at different polymer concentrations. It was observed that upon increasing the polymer concentration from 10 to 20 wt%, the porosity of membrane decreased from 93 to 85%. This can be explained by the fact that increasing the polymer concentration increases the nucleation density. The high nucleation density of membrane decreases the interconnectivity between pores as shown in Fig. 3, hence rendering to the low porosity. However, membranes with higher nucleation density are stronger and have higher integrity structure because they contain a large number of pores with compact arrangement as reported by Khayet and Matsuura, thus indicating that membrane (C) and (B) are stronger compared to membrane (A) [20]. The effects of polymer concentration on nucleation density have been discussed by Akbari, Yegani, and Ferrer [23,24]. The reports indicate that the morphology of membrane was obviously influenced by the polymer concentration, especially on the porosity of polyethylene membranes fabricated via TIPS method.

3.1.2. Effect of quenching temperature on the morphology and porosity of membrane

In order to investigate the effect of quenching temperature, the concentration of polymer was fixed at 15 wt%. Fig. 4 exhibits the effect of quenching temperature on the final morphology of membrane at 15 wt% polymer concentration. From the quality of view, membrane (A) is well-structured and has a perfect shape of pores throughout the membrane, which might be due to adequate time for the formation of membrane pore. However, there was a slightly defective structure detected on membrane (B) due to the entrapment of air bubbles within the matrix. This is supported by Ferrer, who stated that the presence of defect within the structure of membrane is due to the solidification of mixed and entrapped air bubbles [23]. The blocked air bubbles in the pore of membrane fail to diffuse out due to the high cooling rate during solidification. Besides, high cooling rate upon solidification leads to imperfect pore shape due to insufficient time for the formation of pore in the membrane.

Table 4 represents the pore size value of membrane at different quenching temperatures. Apparently, membrane (B) has smaller pore size value compared to membrane (A) due to the nucleation phenomenon. Quenching the membrane at low temperature induces polymer crystallization, which occurs immediately after the phase separation and results in reduced time for droplet growth rate in L–L phase region. Similar results were discussed by Ramaswamy et al. in the study of poly (ECTFE) membranes fabrication via TIPS [25]. As a result, membrane with smaller pore size is produced. However, quenching at high temperature enhances the mobility of polymer chain in polymer diluent solution by driving force and providing enough time for polymer crystallization as reported by Tao et al. [26]. According to Ferrer, quenching at low temperature reduces the pore size due to the nucleation phenomenon, whereas quenching at high temperature tends to produce large pores due to the presence of less nuclei and the occurrence of the growth phenomenon [23].
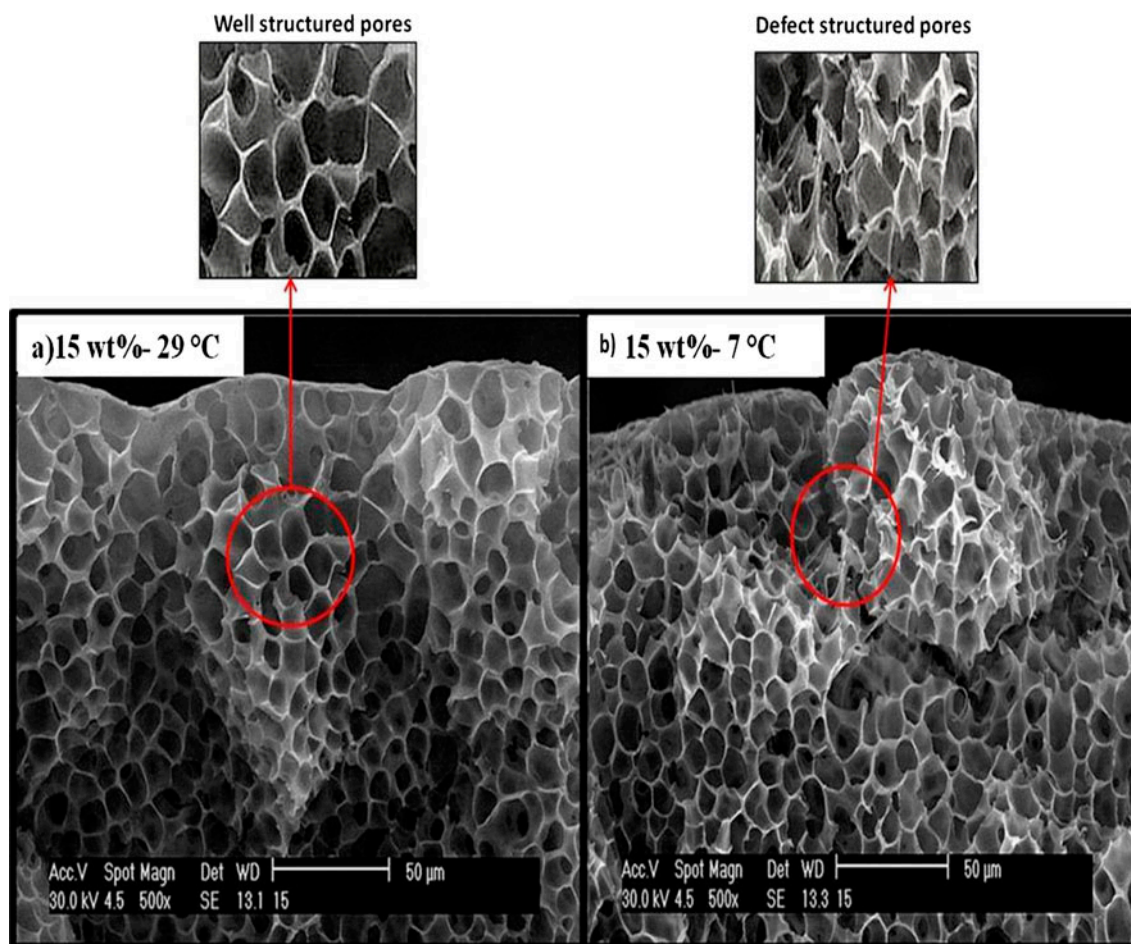
Well structured pores

Defect structured pores

Fig. 4. SEM micrograph of inner cross section of iPP membrane as a function of quenching temperature at 15 wt% polymer concentration: (a) 29℃, (b) 7℃.

Table 4
Pore size and porosity of membrane with 15 wt% polymer concentration at different quenching temperature

Membrane	Quenching temperature (℃)	Pore size (μm)	Porosity (%)
(a)	29	11.5	87
(b)	7	10.3	85

Table 4 exhibits the porosity of the membrane at different quenching temperatures. It shows that the increase in quenching temperature increases membrane porosity. Apparently, the porosity value of the membrane quenched at 29℃ is slightly higher than the membrane quenched at 7℃. This result can be explained by the fact that when the quenching temperature increases, the cooling rate decreases, hence the pores have sufficient time to grow completely and leafy structure of membrane is created. The result is in agreement with Akbari and Yegani in the study of the impact of polymer concentration and coagulation bath temperature [24]. Hence, an increment in pore size and space between pores lead to the high porosity of membrane. However, the porosity values for both membranes did not differ much from each other.

3.2. Performance of fabricated membrane in SLM process

The fabricated membrane produced using TIPS method was used as a support for liquid membrane in SLM process. The removal and recovery of Red 3BS dye were evaluated throughout time. From these values, the ability and performance of fabricated membrane as a support for SLM process were determined.

3.2.1. Suitability of fabricated PP membrane as the support material for SLM

A blank experiment has been carried out in order to find out the possibility of fabricated PP as a

membrane support. In this experiment, no transportation of Red 3BS was observed, which indicates the possibility of using this fabricated membrane as a support liquid membrane as it did not assist the transportation process. Therefore, to assist the transportation of dyes, fabricated membrane support was impregnated in a liquid membrane. Liquid membrane contained TDA and SA in kerosene with the concentration stated in previous research [6].

3.2.2. Performance of membrane with 10 wt% polymer concentration

Fig. 5(a) and (b) exhibit the performance of removal and recovery of Red 3BS using 10 wt% polymer concentration membrane quenched at 29 and 7°C, respectively. In Fig. 6, it was observed that the percentage of removal increased rapidly to 92%, whereas in Fig. 7, the percentage of extraction achieved almost 69% within 90 min. Membrane (a) demonstrated high performance compared to membrane (B) due to high porosity and pore size, hence improving the separation of Red 3BS. Membranes with low polymer concentration have high porosity due to the high interconnectivity of the membrane as discussed in Section 3.1.1. According to Miloud, the interconnection between pores has been identified to significantly affect the permeability of solutes [27]. Besides, large pore sizes of membrane are preferable in the SLM system because large amounts of organic liquid can be retained in the membrane. Thus, diffusion of the desired solute will increase because large amounts of carriers in the organic liquid will bind with the solute and thus will transfer through the membrane.

However, further increase in the extraction time, the volume of feed and the strip solution tends to fluctuate the extraction process. At this moment, both membranes might suffer from the breakage problem. Membrane (a) broke after 90 min of extraction, whereas membrane (B) broke after 120 min of extraction. It was found that membrane (A) experienced breakage earlier than membrane (B) due to the higher porosity compared to membrane (B). The membrane with higher porosity exhibits lower mechanical strength and tends to crack, which reduces the membrane performance. The percentage of extraction and recovery decreased significantly after experiencing rupture on the surface of the membrane. During breakage, the liquid membrane inside the pore membrane is washed out and replaced by the aqueous phase in the pores of the membrane support, hence decreasing the efficiency of removal and recovery as shown in Fig. 6.

The results seem to explain that membrane with 10 wt% polymer concentration does not have sufficient strength for the SLM process since it tends to break and results in the failure of the process. From the visual observation, the volume of the feed phase depleted after the membrane rupture due to the high flow rate of the feed phase and repelled the feed phase solution into the strip phase. Besides, the colors of both phases also changed due to the transfer of solutions.
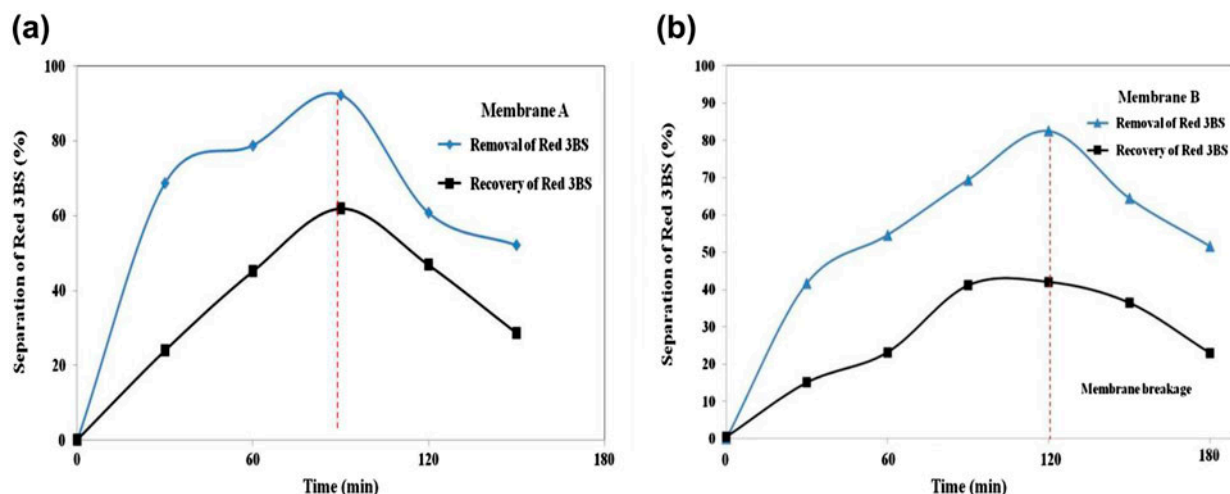

Fig. 5. Performance of removal and recovery of Red 3BS using fabricated membrane support with 10 wt% polymer concentration quench (a) at 29°C, (b) 7°C (Experimental condition: Red 3BS: 50 ppm, TDA = 0.1 M, SA = 0.1 M, NaOH = 0.1 M).
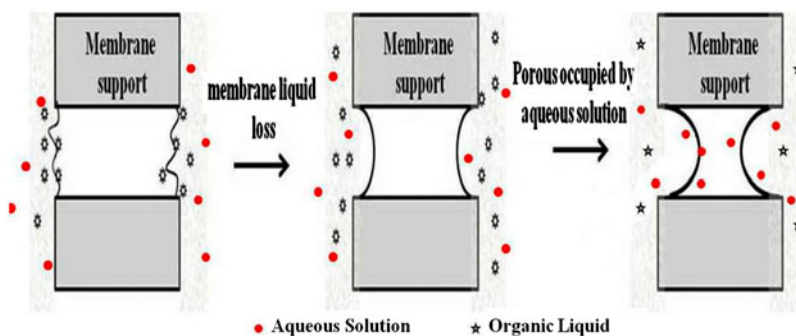
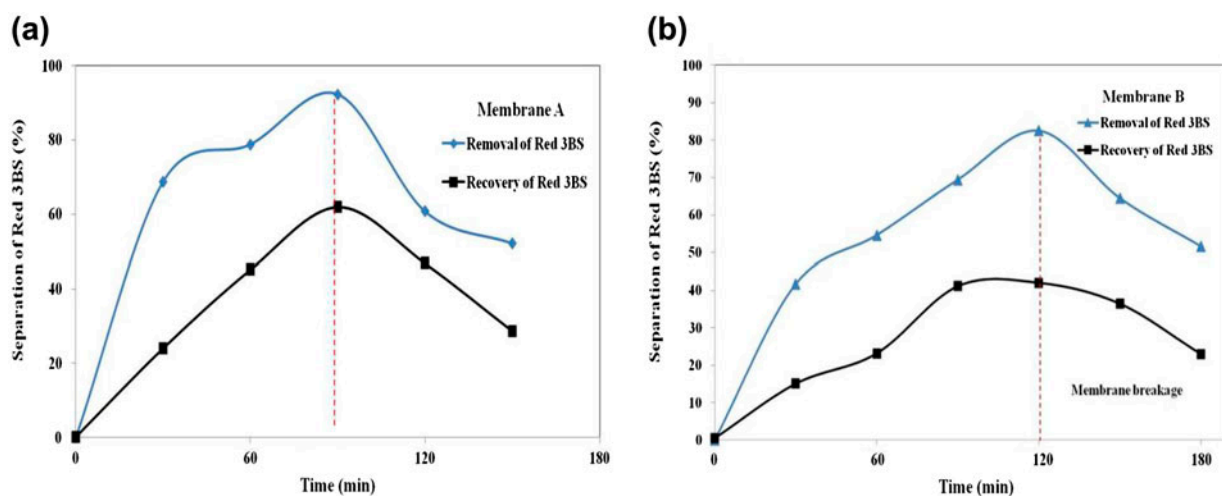Fig. 6. Mechanism of instability of membrane support.

Fig. 7. Performance of removal and recovery of Red 3BS using fabricated membrane support with 15 wt% polymer concentration quench at (a) 29°C, (b) 7°C (Experimental condition: Red 3BS = 50 ppm (pH 3), TDA = 0.1 M, SA = 0.1 M, NaOH = 0.1 M).

3.2.3. Performance of membrane with 15 wt% polymer concentration

Fig. 7(a) and (b) show the performance of removal and recovery of Red 3BS using 15 wt% of polymer concentration quenched at 29 and 7°C, respectively. Meanwhile, Figs. 8 and 9 show the concentration time profile of Red 3BS using 15 wt% of polymer concentration quenched at 29 and 7°C, respectively. It was observed that the percentage of extraction for membrane (A) and membrane (B) increased drastically, with 77 and 72% of removal within 30 min of extraction, respectively. At this point, the concentration of Red 3BS in feed phase reduced drastically from 50 to 18 ppm for membrane (A) and 21 ppm for membrane (B) as shown in Figs. 10–12, respectively. This noticeable increase may be explained by the fact that at this stage, there are many empty pores that are still not filled with the dye ions. This condition enhances the
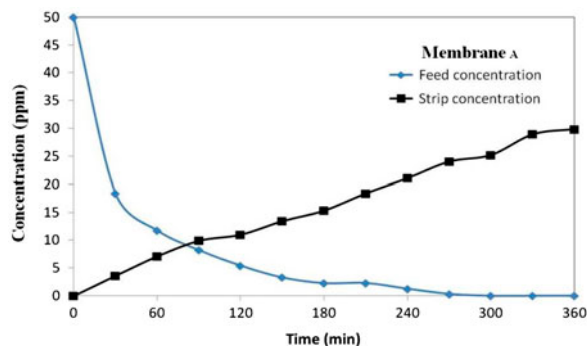

Fig. 8. Concentration of Red 3BS in feed and strip for 360 min using fabricated membrane support with 15 wt% polymer concentration quench at 29°C (Experimental condition: Red 3BS = 50 ppm (pH 3), TDA = 0.1 M, SA = 0.1 M, NaOH = 0.1 M).
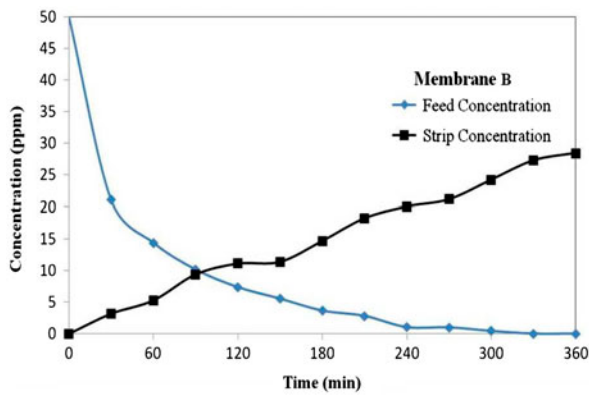
Fig. 9. Concentration of Red 3BS in feed and strip for 360 min using fabricated membrane support with 15 wt% polymer concentration quench at 7°C (Experimental condition: Red 3BS = 50 ppm (pH 3), TDA = 0.1 M, SA = 0.1 M, NaOH = 0.1 M).

permeation rate of dye ions into pores. After 60 min of extraction, the removal for both membranes increased gradually until 100% removal within 360 min of extraction. Both membranes performed well in the extraction process by successfully removing all dye ions within the time given. For recovery performance, it can be observed that the percentage of recovery for both membranes increased gradually with time as shown in Fig. 7(a) and (b). Membrane (a) exhibited high percentage of recovery with around 58% of Red 3BS was recovered. The remaining 42% of

dye ions accumulated and trapped in the pores of the membrane. Meanwhile for membrane (B), 56% of Red 3BS was recovered and around 44% of dye ions were still remained and accumulated in membrane pores. The clogging phenomena occur due to the instability of membrane support and liquid membrane. The membrane support should have high hydrophobicity and well-interconnected pores [28]. Unconnected pores can cause the accumulation of the dye ions inside the membrane. The stability of membrane support can be enhanced by applying dense gelation layer at the interface of feed phase. Gelation layer can be formed by chemical cross-linking with the polymer support. Neplenbroek et al. found that gelation technique could enhance the stability of SLM process for up to 80 weeks [29].

Mass balance for the transported dye in membrane (A) and (B) are shown in Eqs. (6)–(9) below:

For membrane (A)

$$C_{feed} = C_{strip} + C_{accumulate\ in\ pore} \qquad (6)$$

$$50\ ppm_{feed} = 30\ ppm_{strip} + 20\ ppm_{accumulate\ in\ pore} \qquad (7)$$

For membrane (B)

$$C_{feed} = C_{strip} + C_{accumulate\ in\ pore} \qquad (8)$$

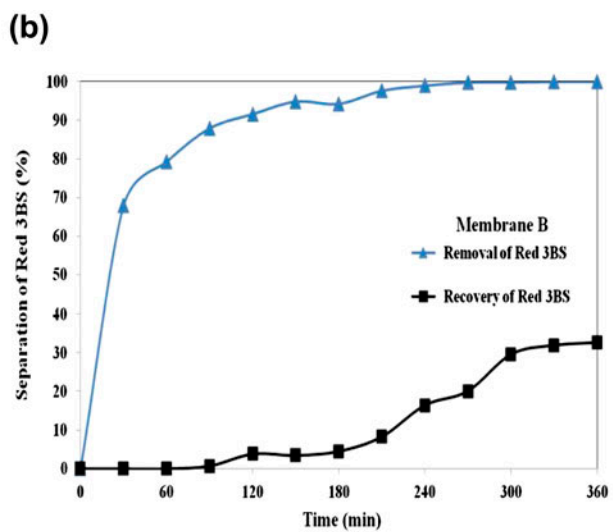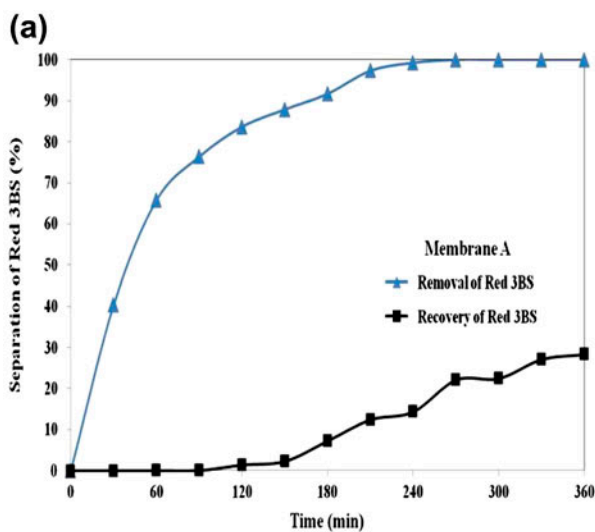$$50\ ppm_{feed} = 28\ ppm_{strip} + 22\ ppm_{accumulate\ in\ pore} \qquad (9)$$

Fig. 10. Performance of removal and recovery of Red 3BS using fabricated membrane support with 20 wt% polymer concentration quench (a) 29°C, (b) 7°C (Experimental condition: Red 3BS = 50 ppm, TDA = 0.1 M, SA = 0.1 M, NaOH = 0.1 M).

From the mass balance in equation it is identified that some dyes have been clogged in the pores of the membrane. This blockage occurs mainly due to the high concentration of polymer, which leads to the enhancement of membrane mechanical resistance, thus increasing the permeation resistance of the solute. As a consequence, solutes failed to diffuse out to the strip phase and become stuck in the pores of the membrane. However, membrane (A) shows good performance in the recovery of dye ions compared to membrane (B) due to the high porosity and pore size of the membrane. The high porosity of the membrane has well-interconnected pores, which provide a continuous path for the movement of dye ions assisted by the carrier from the feed phase to the strip phase. Hence, this reduces the occurrence of accumulation and enhances the recovery of dye ions. According to Le-Clech et al. small pore size of the membrane hinders the transport of solute and induces fouling problem [30]. In this case, the fouling problem refers to the accumulation of dye ions on the surface of membrane, which restricts the removal and recovery of dye ions processes.

In addition, the permeability values for both membranes are also presented in Table 5. It was found that membrane (A) exhibited good performance of extraction with higher permeability value, 103 cm^3/cm^2 min compared to membrane (B) with a permeability value of 94 cm^3/cm^2 min. The result indicates that the permeation of Red 3BS ions through the pores of membrane (A) was higher and easier than membrane (B), which might be due to the well-structured and interconnected pores of membrane (A). As discussed earlier in the previous section, according to Miloud, permeability is highly dependent on the interconnected pores within a membrane [27].

3.2.4. Performance of membrane with 20 wt% polymer concentration

Fig. 10(a) and (b) illustrate the percentage of removal and recovery of Red 3BS using 20 wt%

polymer concentrations quenched at (a) 29 and (b) 7°C, respectively. Meanwhile, Figs. 11 and 12 show the concentration time profile of Red 3BS using 20 wt % of polymer concentration quenched at 29 and 7°C, respectively. It was observed that the removal percentage for membrane (A) and (B) increased significantly to 65 and 79%, respectively, within 60 min of extraction. At this point, the concentration of Red 3BS in the feed phase dropped drastically to 17 ppm for membrane (A) and 10 ppm for membrane (B) as shown in Figs. 11 and 12. Further increase in the extraction time resulted in a gradual increase in the removal efficiency until the efficiency achieved 100% after 360 min.

For recovery process, it can be observed that both membranes exhibited low performance of recovery throughout the time. In the first 90 min, no recovery of dye ions was observed for both membranes. At this point, the possibility of diffusion of dye ions into the pores of a membrane is low due to the compact arrangement and dense structure of pore membrane. High polymer concentration is likely to produce membrane with low interconnectivity between cellular pores and small pore size as discussed by Wu et al. [21].

Consequently, dye ions hardly diffuse into the membrane, thus reduces the permeation rate of dye ions. However, the dye ions began to recover after 270 min of extraction for both membranes. After 360 min of extraction, only 28% of dye ion was successfully recovered by membrane (A). At this stage, around 72% of Red 3BS still remained and trapped in the pores of membrane support. Meanwhile for membrane (B), only 33% of dye was recovered and

Table 5
Permeability coefficient value of 15 wt% polymer concentration as a function of quenching temperature

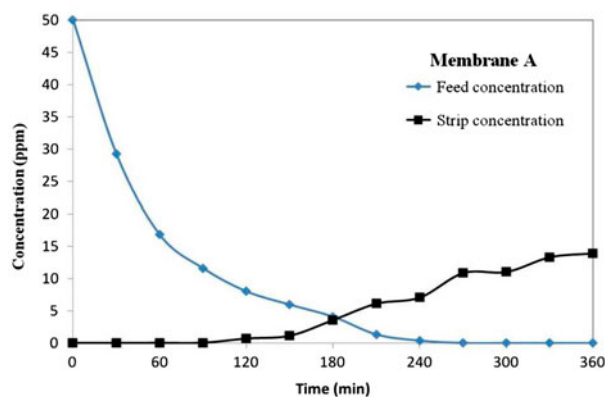| Quenching temperature (°C)	Permeability value ($P \times 10^5$ cm^3/cm^2 min)	
	15 wt%	20 wt%
29	103	104
7	94	128

Fig. 11. Concentration of Red 3BS in feed and strip for 360 min using fabricated membrane support with 20 wt% polymer concentration quench at 29°C (Experimental condition: Red 3BS = 50 ppm (pH 3), TDA = 0.1 M, SA = 0.1 M, NaOH = 0.1 M).
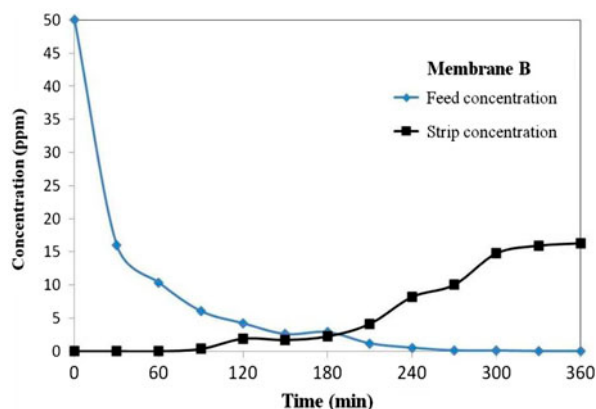
Fig. 12. Concentration of Red 3BS in feed and strip for 360 min using fabricated membrane support with 20 wt% polymer concentration quench at 7°C (Experimental condition: Red 3BS = 50 ppm (pH 3), TDA = 0.1 M, SA = 0.1 M, NaOH = 0.1 M).

67% of dye ions were deposited onto the pore walls, thus reducing the pore size. The reduction of the pore membrane size reduced the permeability of dye ions. As a result, the dye ions were unable to diffuse out and trapped within the pores, which leads to the recovery inefficiency. This is in line with the findings obtained by Lin et al. and Khayet and Matsuura [14,20]. Mass balance for the transported dye for membrane (A) and (B) is shown in Eq. below:

Membrane (A)

$$C_{feed} = C_{strip} + C_{accumulate} \tag{10}$$

$$50\ ppm_{feed} = 14\ ppm_{strip} + 36\ ppm_{accumulate} \tag{11}$$

Membrane (B)

$$C_{feed} = C_{strip} + C_{accumulate} \tag{12}$$

$$50\ ppm_{feed} = 16\ ppm_{strip} + 34\ ppm_{accumulate} \tag{13}$$

At the end of experiment, it was found that the concentrated red precipitation was observed on the surface of membrane support. From the mass balance equation, it stated that almost 36 ppm of dyes was clogged in membrane (A) and 34 ppm in membrane (B). This can be explained by the fact that lots of dye ions clogged the pores and failed to diffuse out of the membrane.

The permeability values for both membranes are presented in Table 5. The permeation rate of dye ions in membrane (B) of 128 cm³/cm² min was higher compared to membrane (A) with the permeability value of 104 cm³/cm² min. This result is in contrast with the earlier explanation, which indicates that the membrane with high porosity leads to the high removal efficiency, but in this case the membrane with lower porosity leads to the high removal efficiency. This might be explained by the presence of many small pores on the surface of membrane near the feed side that can increase the extraction rate, hence increasing the permeability of dye ions through the membrane. However, many of the dye ions failed to diffuse through the membrane due to the unconnected pores in the surface of the membrane near the strip side. As a result, the dye ions accumulated inside the pores of the membrane, which decreased the recovery efficiency.

Overall, it can be concluded that the membrane with 10 wt% polymer concentration was found to be unsuitable as a membrane support due to insufficient tensile strength and integrity structure. The membrane suffers breakage on the membrane surface, which restricts the application of SLM process. Membrane with 20 wt% polymer concentration has successfully removed 100% of Red 3BS from an aqueous solution. However, it reduced the recovery efficiency due to the membrane fouling problem. Membrane fouling is a process where solute or particle deposits onto membrane pores and degrades the membrane performance. In contrast, the fabricated membrane with 15 wt% polymer concentration quenched at 29°C shows excellent performance in SLM process with 100 and 58% of removal and recovery of Red 3BS, respectively, within 6 h. Besides, the membrane remains stable without suffering any rupture on membrane surface during SLM process. Thus, the fabricated membrane with 15 wt% polymer concentration quenched at 29°C is feasible to be used as a membrane support for the removal and recovery of Red 3BS using SLM process.

3.3. Stability of membrane support in SLM process

The SLM process is rarely applied in the industrial scale due to insufficient stability of membrane support. This means that the stability of membrane support is very crucial in SLM process. Therefore, the stability of the fabricated membrane was tested in this study. The fabricated membrane with 15 wt% polymer concentration quenched at 29°C was selected since it provides high performance in the SLM process compared to the other fabricated membranes. The stability of membrane support was examined using the same membrane support repeatedly without further impregnation in liquid membrane. Fig. 13 exhibits the stability of the membrane support of the fabricated

Table 6
Comparison between commercial membrane

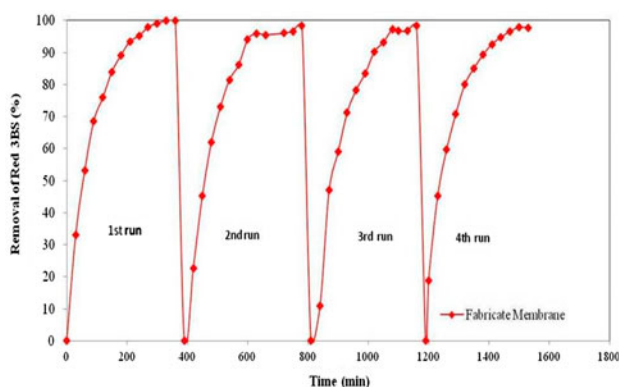| Separation process	Commercial polymeric membrane	Stability membrane support (h)	References
Gas separation (CO_2, H_2, N_2, O_2)	Polyethersulfone	7	[31]
	Nylon, 6	2.5	
	PVDF	2.5	
Acetic acid	Polytetraflouroethane	16	[32]
Copper	Polypropylene celgard 2,500	10.5	[33]

Fig. 13. Stability of membrane support of fabricate membrane with 15 wt% polymer concentration quench at 29°C (Experimental condition: Red 3BS: 50 ppm, TDA = 0.1 M, SA = 0.1 M, NaOH = 0.1 M).

membrane with 15 wt% polymer concentration quenched at 29°C under optimum condition of SLM process. For the fabricated membrane, it was observed that the membrane support remained stable until the fourth run (after 25.5 h) of extraction. The first run required 6 h to completely remove almost 100% of reactive dye from the feed phase. In the second run, the efficiency of the extraction decreased slightly to 99% of reactive dye removed within 6 h of extraction. The third and fourth runs were considered to be stable with high percentage of removal of 98 and 97%, respectively. The process can be considered stable since high percentage of dye removal was achieved even after 25.5 h of continuous run without reimpregnated the membrane support in the liquid membrane. The stability test was stopped after the fourth run although the fabricated membrane still showed high stability performance. Compared to the commercial support used by previous research as shown in Table 6, it was found that the fabricated membrane is more superior in terms of stability and chemical resistance. Therefore, the fabricated membrane support has a big potential to be used in the industrial process and its stability value is found to be sufficient

to meet the operation hour of the textile industrial process since it operates 12 h per day.

It is proven that the fabricated membrane demonstrated high stability in separation of Red 3BS, and performed well as a polymeric support in SLM system. This can be due to the appropriate morphology structure with high tensile strength and chemical resistance.

4. Conclusion

The fabricated PP membrane prepared using TIPS method is proven as an effective membrane support in SLM process for the separation of reactive Red 3BS from an aqueous solution. Almost 100 and 58% of Red 3BS was successfully removed and recovered using 15 wt% polymer concentration (air cooling) as a membrane support, respectively. The fabricated membrane also demonstrated high stability for up to 25.5 h toward the separation process, hence the membrane is feasible to be applied in the industrial scale.

References

[1] N. Mathur, P. Bhatnagar, P. Sharma, Review of the mutagenicity of textile dye products, Univ. J. Environ. Res. Technol. 2 (2012) 1–18.
[2] G.M. Nisola, E. Cho, A.B. Beltran, M. Han, Y. Kim, W.-J. Chung, Dye/water separation through supported liquid membrane extraction, Chemosphere 80 (2010) 894–900.
[3] K. Kadirvelu, M. Kavipriya, C. Karthika, M. Radhika, N. Vennilamani, S. Pattabhi, Utilization of various agricultural wastes for activated carbon preparation and application for the removal of dyes and metal ions from aqueous solutions, Bioresour. Technol. 87 (2003) 129–132.

[4] N. Othman, N. Mili, S.N. Zailani, Emulsion liquid membrane extraction of turquoise blue reactive dye—Study on membrane breakage and swelling, J. Appl. Membr. Sci. Technol. 11 (2010) 43–48.

[5] N. Othman, N. Mili, Y.M. Wong, Liquid–liquid extraction of black B dye from liquid waste solution using tridodecylamine, J. Environ. Sci. Technol. 4 (2011) 324–331.

[6] N. Othman, R. Djamal, N. Mili, S.N. Zailani, Removal of Red 3BS dye from wastewater using emulsion liquid membrane process, J. Appl. Sci. 11 (2011) 1406–1410.

[7] N. Bukhari, M.A. Chaudry, M. Mazhar, Cobalt(II) transport through triethanolamine–cyclohexanone supported liquid membranes, J. Membr. Sci. 234 (2004) 157–165.

[8] M. Chakraborty, D. Dobaria, A.P. Parikh, Performance and stability study of vegetable oil based supported liquid membrane, Indian J. Chem. Technol. 17 (2010) 126–132.

[9] N.M. Kocherginsky, Q. Yang, L. Seelam, Recent advances in supported liquid membrane technology, Sep. Purif. Technol. 53 (2007) 171–177.

[10] A. Figoli, W.F.C. Sager, M.H.V. Mulder, Facilitated oxygen transport in liquid membranes: Review and new concepts, J. Membr. Sci. 181 (2001) 97–110.

[11] G. Arslan, A. Tor, Y. Cengeloglu, M. Ersoz, Facilitated transport of Cr(III) through activated composite membrane containing di-(2-ethylhexyl)phosphoric acid (DEHPA) as carrier agent, J. Hazard. Mater. 165 (2009) 729–735.

[12] P. Dzygiel, P.P. Wieczorek, Supported Liquid Membranes and Their Modifications: Definition, Classification, Theory, Stability, Application and Perspectives, Elsevier, Amsterdam, 2010.

[13] S.S. Fu, H. Matsuyama, M. Teramoto, D.R. Lloyd, Preparation of microporous polypropylene membrane via thermally induced phase separation as support of liquid membrane used for metal ion recovery, J. Chem. Eng. Jpn. 36 (2003) 1397–1404.

[14] Y.K. Lin, G. Chen, J. Yang, X.L. Wang, Formation of isotactic polypropylene membranes with bicontinuous structure and good strength via thermally induced phase separation method, Desalination 236 (2009) 8–15.

[15] N. Othman, S.N. Zailani, N. Mili, Recovery of synthetic dye from simulated wastewater using emulsion liquid membrane process containing tri-dodecyl amine as a mobile carrier, J. Hazard. Mater. 198 (2011) 103–112.

[16] D. de Agreda, D.I. Garcia, F.A. Lopes, F.J. Alguacil, Supported liquid membranes technologies in metals removal from liquid effluents, Revista De Metalurgia 47 (2011) 146–168.

[17] J. Lv, Q. Yang, J. Jiang, T.S. Chung, Exploration of heavy metal ions transmembrane flux enhancement across a supported liquid membrane by appropriate carrier selection, Chem. Eng. Sci. 62 (2007) 6032–6039.

[18] Q. Yang, T.S. Chung, Y. Xiao, K. Wang, The development of chemically modified P84 Co-polyimide membranes as supported liquid membrane matrix for Cu

[19] S.S. Fu, H. Mastuyama, M. Teramoto, Ce(III) recovery by supported liquid membrane using polyethylene hollow fiber prepared via thermally induced phase separation, Sep. Purif. Technol. 36 (2004) 17–22.

[20] M. Khayet, T. Matsuura, Membrane Distillation: Principles and Applications, Elsevier, Netherlands, 2011.

[21] Q.-Y. Wu, L.-S. Wan, Z.-K. Xu, Structure and performance of polyacrylonitrile membranes prepared via thermally induced phase separation, J. Membr. Sci. 409–410 (2012) 355–364.

[22] Y. Sun, L. Saleh, B. Bai, Measurement and impact factors of polymer rheology in porous media, Intech Open Science, 2012 pp. 187–202. Available from: <http://www.intechopen.com/books/rheology/polymer-rheology-in-porous-media>

[23] M.C.H. Ferrer, Development and Characterisation of Completely Degradable Composite Tissue Engineering, Polytechnic University, Catalonia, 2007.

[24] A. Akbari, R. Yegani, Study on the impact of polymer concentration and coagulation bath temperature on the porosity of polyethylene membranes fabricated via TIPS method, J. Membr. Sep. Technol. 1 (2012) 100–107.

[25] S. Ramaswamy, A.R. Greenberg, W.B. Krantz, Fabrication of poly (ECTFE) membranes via thermally induced phase separation, J. Membr. Sci. 210 (2002) 175–180.

[26] H. Tao, J. Zhang, X. Wang, J. Gao, Phase separation and polymer crystallization in a poly (4-methyl-1-pentene)-dioctylsebacate-dimetylphtalate system via thermally induced phase separation, J. Polym. Sci. 45 (2006) 153–161.

[27] B. Miloud, Permeability and porosity characteristics of steel fiber reinforced concrete, Asian J. Civ. Eng. (Build. Hous) 6 (2005) 317–330.

[28] K. Parhi, Supported liquid membrane principle and its practices: A short review, J. Chem. (2013) 2–11. Available from: <http://www.hindawi.com/journals/jchem/2013/618236/>.

[29] A.M. Neplenbroek, D. Bargeman, C.A. Smolders, The stability of supported liquid membranes, Desalination 79 (1990) 303–312.

[30] P. Le-Clech, V. Chen, T.A.G. Fane, Fouling in membrane bioreactors used in wastewater treatment, J. Membr. Sci. 284 (2006) 17–53.

[31] Y. Zhao, C. Qiu, X. Li, A. Vararattanavech, W. Shen, J. Torres, C. Hélix-Nielsen, R. Wang, X. Hu, A.G. Fane, C.Y. Tang, Synthesis of robust and high-performance aquaporin-based biomimetic membranes by interfacial polymerization-membrane preparation and RO performance characterization, J. Membr. Sci. 423–424 (2012) 422–428.

[32] J. Narayanan, K. Palanivelu, Recovery of acetic acid by supported liquid membrane using vegetable oils as liquid membrane, Indian J. Chem. Technol. 15 (2008) 266–270.

[33] H.-D. Zheng, B.-Y. Wang, Y.-X. Wu, Q.-L. Ren, Instability mechanisms of supported liquid membranes for copper (II) ion extraction, Colloids Surf. A 351 (2009) 38–45.